NUSC Technical Document 9015
9 December 1991

Mode Transition Matrix for Multimode Optical Fiber Systems

Thomas J. Gryk
Submarine Electromagnetic
Systems Department

Naval Underwater Systems Center
Newport, Rhode Island • New London, Connecticut

PREFACE

This report was funded under NUSC Project No. A51090, "F.O. Measurements Techniques," principal investigator T.J. Gryk (Code 3422). The sponsoring activity is the Office of Naval Technology, program manager CDR A. Baivier.

The technical reviewer for this report was G. E Holmberg (Code 3422).

REVIEWED AND APPROVED: 9 December 1991

D. VICCIONE
Head, Submarine Electro-Magnetic Systems Department

REPORT DOCUMENTATION PAGE

Form Approved
OMB No. 0704-0188

1. AGENCY USE ONLY (Leave blank)	2. REPORT DATE	3. REPORT TYPE AND DATES COVERED
	9 December 1991	

4. TITLE AND SUBTITLE

Mode Transition Matrix for Multimode Optical Fiber Systems

5. FUNDING NUMBERS

PE: 62233N

6. AUTHOR(S)

T. J. Gryk

7. PERFORMING ORGANIZATION NAME(S) AND ADDRESS(ES)

Naval Underwater Systems Center
New London, CT 06320

8. PERFORMING ORGANIZATION REPORT NUMBER

NUSC TD 9015

9. SPONSORING/MONITORING AGENCY NAME(S) AND ADDRESS(ES)

Officer of Naval Technology
Arlington, VA 22217

10. SPONSORING/MONITORING AGENCY REPORT NUMBER

11. SUPPLEMENTARY NOTES

12a. DISTRIBUTION/AVAILABILITY STATEMENT

Approved for public release and distribution is unlimited.

12b. DISTRIBUTION CODE

13. ABSTRACT (Maximum 200 words)

This report discusses the Mode Transition Matrix formalism for determining the loss exhibited by a multimode, passive fiber optic component. This report presents a theoretical discussion of the technique including a detailed description of the approximations made by the matrix formalism.

The report experimentally verifies that the modal properties of passive components can be described using a two-dimensional matrix. This matrix description allows an accurate prediction of the device's loss when incorporated in a concatenation with other fiber optic components.

Finally, the report introduces an invention which allows the mode transition matrix to be determined quickly and accurately. This invention uses fiber optic switches and mode filters to determine the transition matrix and therefore does not require a measurement of the fiber's near field pattern.

14. SUBJECT TERMS

Transfer matrix
Modal power distribution
Near field pattern

15. NUMBER OF PAGES

55

16. PRICE CODE

17. SECURITY CLASSIFICATION OF REPORT	18. SECURITY CLASSIFICATION OF THIS PAGE	19. SECURITY CLASSIFICATION OF ABSTRACT	20. LIMITATION OF ABSTRACT
UNCLASSIFIED	UNCLASSIFIED	UNCLASSIFIED	UNLIMITED

CONTENTS

LIST OF ILLUSTRATIONS

INTRODUCTION

Multimode fiber op' 'c components are primarily used in short-haul communications systems. Standard loss measurement techniques do not accurately predict a multimode component's performance when utilized in a Local Area Network (LAN) because these methods do not account for the mode dependent losses which are often exhibited by multimode devices. Various techniques have been introduced to provide an approximate description of the modal characteristics of these components and include: differential mode attenuation[1], mode transition matrix[2], and mode transfer function[3]. The transition matrix formalism is described in the next section of this report, while a detailed discussion of the other methods is presented in the section entitled, "Alternative Approximation Techniques."

Much attention has been given to the Mode Transition Matrix (MTM) method. Holmes[2] introduced the technique in 1980 and it has since been successfully applied to quasi-step-index fibers[4], multimode fiber transmission[5], and graded index fusion splices[6]. Gabriel[7] rigorously discussed the mode block matrix formalism; generalizing the technique to allow for other basis sets including Chebychev and Jacobi polynomials, and Gryk, et al.[8] investigated the sensitivity of the matrix elements to variations of the input launch conditions. While the technique offers a more complete description of a passive

fiber optic component's performance than standard loss measurements, the method is inherently complicated since it relies on a determination of the modal power distribution (MPD) as well as the total optical power. It was the purpose of the present work to remove the complications associated with the determination of the Mode Transition Matrix, and develop a quick, non-destructive test technique which accurately predicts the performance of these passive fiber optic devices when utilized in a Local Area Network.

THEORY

Modal Power Distribution

The optical power propagating in a multimode optical fiber is distributed between the various modes of the fiber. The modal power distribution, $P(\delta,\nu)$, gives a complete description of the optical power carried by each guiding fiber mode. Grau and Leminger[9] derive a relationship between the modal power distribution and the near field pattern, $N(r)$, for axially symmetric fibers in the mode continuum approximation:

$$N(r)=2\left(\frac{n_1 k_0}{\pi}\right)^2\int_{g(s)\Delta}^{\Delta} d\delta\int_0^{R(r,\delta)}\left[R^2(r,\delta)-\nu^2\right]^{-1/2}P(\delta,\nu)\,d\nu \tag{1}$$

where,

$$R(r,\delta)=V\frac{r}{a}\left[\frac{\delta}{\Delta}-g\left(\frac{r}{a}\right)\right]^{1/2} \tag{1a}$$

s is the normalized radius, $g(s)$ is the refractive index profile, V is the fiber's V-number, k_0 is the free-space wavenumber, n_1 is the index of refraction along the axis of the fiber, Δ is the refractive index contrast, δ is the propagation constant, and ν is the azimuthal mode number. If the MPD is assumed to be only a function of δ then the total power is found by integrating the MPD,

$$P_{tot}=\int_0^{\Delta} P(\delta)\,m(\delta)\,d\delta \tag{2}$$

where $m(\delta)$ is the mode density as given by Leminger and Grau[10] integrated over ν. For parabolic index profiles, the

density of modes is given by

$$m(\delta) = \frac{V^2}{2\Delta^2}\delta \qquad (3)$$

These results assume a mode continuum approximation (the MPD is considered to be a continuous function of continuous mode parameters) since the phase of the light has been ignored during the measurement of the near field pattern. In other words, these results are only valid for incoherent light, or if they are interpreted as the average over all possible speckle patterns for coherent light. Mickelson and Eriksrud[11] discuss the mode continuum approximation in detail and determine the range of linewidths for which the modes form a continuum for a parabolic index profile to be:

$$\frac{\delta\lambda}{\lambda} > \frac{\sqrt{2\Delta}}{a k_0 n_g} \qquad (4)$$

where n_g is the effective group index. For a typical 100/140μm fiber the source linewidth must on the order of 0.25nm. This is not very restrictive since most fiber optic sources, excluding narrow linewidth distributed feedback laser diodes and the like, will generally exhibit linewidths on the order of a few nanometers.

Although the near field pattern is uniquely determined by the modal power distribution, it can be shown[11] that the converse is not true. Therefore, an assumption as to the form of the MPD must be made if the MPD is to be determined from a set of near field pattern data. One possible, and often used, simplification requires the modal power distribution to be

independent of the azimuthal mode number, ν. Then a unique determination of the MPD can be made from the near field pattern and is given by:

$$P(\delta) = \frac{-\pi a}{\Delta (n_1 k_0)^2} \frac{dN(r)}{dr} \frac{1}{dg(s)/ds} \quad \text{evaluated at} \quad \frac{\delta}{\Delta} = g(s) \tag{5}$$

For parabolic index profiles, this reduces to:

$$P(\delta) = \frac{-\pi a^2}{2 \Delta (n_1 k_0)^2} \frac{1}{r} \frac{dN(r)}{dr} \tag{6}$$

Mode Power Vector

The modal power distribution can be written as a linear combination of an orthogonal, complete set of functions, $\phi_j(\delta)$,

$$P(\delta)\, m(\delta) = \sum_j c_j\, \phi_j(\delta) \tag{7}$$

where the coefficients are given by

$$c_j = \frac{1}{A_j^2} \int_0^{\Delta} P(\delta)\, m(\delta)\, \phi_j(\delta)\, d\delta \tag{8}$$

The functions, $\phi_j(\delta)$, are not normalized. The set of normalization constants are given by

$$A_j^2 = \int_0^{\Delta} \phi_j^2(\delta)\, d\delta \tag{9}$$

If the basis functions are not orthogonal, the coefficients must be determined by simultaneously solving a set of linear equations of the form

$$\int_0^{\Delta} P(\delta)\, m(\delta)\, \phi_j(\delta)\, d\delta = \sum_n c_n \left(\int_0^{\Delta} \phi_n(\delta)\, \phi_j(\delta)\, d\delta \right) \tag{10}$$

For the purposes of this investigation, however, an orthogonal basis is assumed. The modal power distribution can be described as a mode power vector, whose elements are given by:

$$\overline{P} = (P_1, P_2, \ldots, P_j, \ldots P_\infty) \text{ such that } P_j = c_j A_j^2 \tag{11}$$

If we choose a normalization for our basis set such that

$$\int_0^\Delta \phi_j(\delta)\, d\delta = A_j^2 \tag{12}$$

then the total power can be written in the form:

$$P_{tot} = \sum_j P_j \tag{13}$$

Mode Transition Matrix

The modal coupling of a passive fiber optic component can be described by the transformation

$$P^{o}(\delta)\, m(\delta) = \int_{0}^{\Delta} T(\delta,\delta')\, P^{i}(\delta')\, m(\delta')\, d\delta' \tag{14}$$

where $P^{i}(\delta)m(\delta)$ and $P^{o}(\delta)m(\delta)$ describe the MPD entering and exiting the component, respectively. Inserting equation (7) for the modal power distributions of equation (14), we get:

$$\sum_{j} c_{j}^{o}\, \phi_{j}(\delta) = \sum_{j} c_{j}^{i} \left(\int_{0}^{\Delta} T(\delta,\delta')\, \phi_{j}(\delta')\, d\delta' \right) \tag{15}$$

Multiplying each side by $\phi_{k}(\delta)$ and integrating over δ yields:

$$P_{k}^{o} = \sum_{j} P_{j}^{i} \left(\frac{1}{A_{j}^{2}} \int_{0}^{\Delta} \phi_{k}(\delta)\, T(\delta,\delta')\, \phi_{j}(\delta')\, d\delta\, d\delta' \right) \tag{16}$$

which can be written as a matrix equation of the form:

$$\bar{P}^{o} = \bar{\bar{T}} \cdot \bar{P}^{i} \tag{17}$$

where the matrix elements are given by:

$$T_{kj} = \frac{1}{A_{j}^{2}} \int_{0}^{\Delta} \int_{0}^{\Delta} \phi_{k}(\delta)\, T(\delta,\delta')\, \phi_{j}(\delta')\, d\delta\, d\delta' \tag{18}$$

and $\bar{P}^{i}$ and $\bar{P}^{o}$ are the aforementioned mode power vectors determined at the input and output of the fiber optic component, respectively. The mode transition matrix, $\bar{\bar{T}}$,

described in this fashion is completely equivalent to the mode transfer function $T(\delta,\delta')$. Unfortunately it is of infinite dimension, and therefore a solution to the matrix equation (17) can not be determined.

Finite Element Matrix

The matrix of equation (18) is of infinite dimension, and as such, is of little practical importance. If we assume, however, that the modal power distribution can be approximated by a finite sum of N orthogonal functions then the mode transfer function is approximately described by an NxN matrix. For simplicity, we may assume the expansion of the modal power distribution to be truncated after only two functions.

$$P(\delta)\, m(\delta) \approx c_1\, \phi_1(\delta) + c_2\, \phi_2(\delta) \tag{19}$$

The mode transition matrix is then given by the 2x2 matrix:

$$\overline{\overline{T}} = \begin{bmatrix} T_{11} & T_{12} \\ T_{21} & T_{22} \end{bmatrix} \tag{20}$$

The four independent elements can now be uniquely determined by measuring the two sets of input and output modal power distributions. If we denote the independent measurement sets by P(a) and P(b), then equation (17) yields a set of linear equations of the form

$$\overline{P}^{o}(a) = \overline{\overline{T}} \cdot \overline{P}^{i}(a) \;:\; \overline{P}^{o}(b) = \overline{\overline{T}} \cdot \overline{P}^{i}(b) \tag{21}$$

This set can be written as a single matrix equation

$$\overline{\overline{P}}^{o} = \overline{\overline{T}} \cdot \overline{\overline{P}}^{i} \quad \text{where } \overline{\overline{P}}^{o} = \begin{bmatrix} P_1^o(a) & P_1^o(b) \\ P_2^o(a) & P_2^o(b) \end{bmatrix} \text{ and } \overline{\overline{P}}^{i} = \begin{bmatrix} P_1^i(a) & P_1^i(b) \\ P_2^i(a) & P_2^i(b) \end{bmatrix} \tag{22}$$

whose solution is given by

$$\overline{\overline{T}} = \overline{\overline{P}}^{o} \cdot (\overline{\overline{P}}^{i})^{-1} \tag{23}$$

It is obvious that the inverse of $\overline{\overline{P}}^{i}$ must exist for the transition matrix to be determined. Therefore, the determinant of $\overline{\overline{P}}^{i}$ must not vanish.

$$\det(\overline{\overline{P}}^{i}) = P_1^i(a)\,P_2^i(b) - P_1^i(b)\,P_2^i(a) \neq 0 \tag{24}$$

This requires that the two sets of modal power distributions used to calculate $\overline{\overline{T}}$ must have been for linearly independent input MPDs. Although this method could theoretically be extended to a matrix of very large dimension, diffraction limitations restrict the number of suitably independent input conditions to only a few (2 or 3). Unrau[12] suggests that a 2x2 matrix should be sufficient to describe the modal properties of many fiber optic components and is therefore the focus of this investigation.

Step Function Basis

Orthogonal step functions form a physically descriptive basis set. Considering the 2x2 matrix aforementioned, the two orthogonal step functions can be written:

$$\phi_1 = \begin{cases} 1, & \delta<\delta_o \\ 0, & \delta>\delta_o \end{cases}, \qquad \phi_2 = \begin{cases} 0, & \delta<\delta_o \\ 1, & \delta>\delta_o \end{cases} \tag{25}$$

The mode power vector is then given by:

$$P_1 = \int_0^{\delta_o} P(\delta)\, m(\delta)\, d\delta, \quad P_2 = \int_{\delta_o}^{\Delta} P(\delta)\, m(\delta)\, d\delta \tag{26}$$

Physically, this basis set integrates the modal power distribution into low- and high-order mode blocks. P_1 is the total power contained in all the modes of propagation constant $\delta<\delta_o$, while P_2 contains all the power propagating in modes of propagation constant $\delta>\delta_o$. The mode transition matrix elements of equation (20) calculated using this basis can then be interpreted as mode block coupling coefficients, where T_{11} describes low- to low-order mode block coupling, T_{12} describes high- to low-order mode mode block coupling, T_{21} describes low- to high-order mode block coupling, and T_{22} describes high- to high-order mode block coupling. This physically meaningful interpretation restricts the range of each coefficient to be between 0 and 1. The major limitation of this basis set lies in its inability to accurately describe the modal power distribution, as was assumed in

equation (19). The method still has merit, however, if it is assumed that the transfer function of equation (14) does not distinguish between modes in the same mode block. In other words, the transfer function must be assumed to be of the form:

$$T(\delta,\delta') = \left\{ \begin{array}{ll} T_{11} & \delta<\delta_o,\ \delta'<\delta_o \\ T_{12} & \delta<\delta_o,\ \delta'>\delta_o \\ T_{21} & \delta>\delta_o,\ \delta'<\delta_o \\ T_{22} & \delta>\delta_o,\ \delta'>\delta_o \end{array} \right\} \qquad (27)$$

so that the transfer equation (14) can be written as a matrix equation regardless of the form of the modal power distribution. This is the assumption made by Holmes[2] and others who have used mode blocks to calculate the mode transition matrix, and its validity for each passive fiber optic component must be determined from experiment.

Standardization

The Mode Transition Matrix method is well understood and attempts have been made to standardize some of the assumptions made and procedures used to calculate the MTM of a fiber optic component. Until this section, the theory of the MTM has been dealt with in as much generality as possible, but the following sections require the use of these standardizing assumptions. Therefore, these "standards" are listed here and are assumed in all subsequent discussion of the mode transition matrix.

1. The Mode Transition Matrix will be assumed to be a 2x2 matrix of the form of equation (27) where the cutoff mode value will be given by: $\delta_o = 0.5\Delta$.
2. The independent launch conditions to be used will consist of an underfilled launch (small-spot) excitation, and an overfilled launch (power in all guided modes).
3. For the purposes of all calculations involving the modal power distribution, the refractive index profile is assumed to be parabolic.
4. The modal power distribution is only a function of the propagation constant, δ. Optical power is uniformly distributed between azimuthal modes with the same propagation constant.

EXPERIMENTAL DETAILS AND CONSIDERATIONS

Near Field Pattern Measurements

Assuming the modal power distribution is strictly a function of the propagation constant, $P(\delta,\nu)=P(\delta)$, then the modal power distribution of a parabolic-index optical fiber can be determined from the measured near field pattern using equation (6). The near field pattern can be measured using a CCTV camera as illustrated in Figure 1.

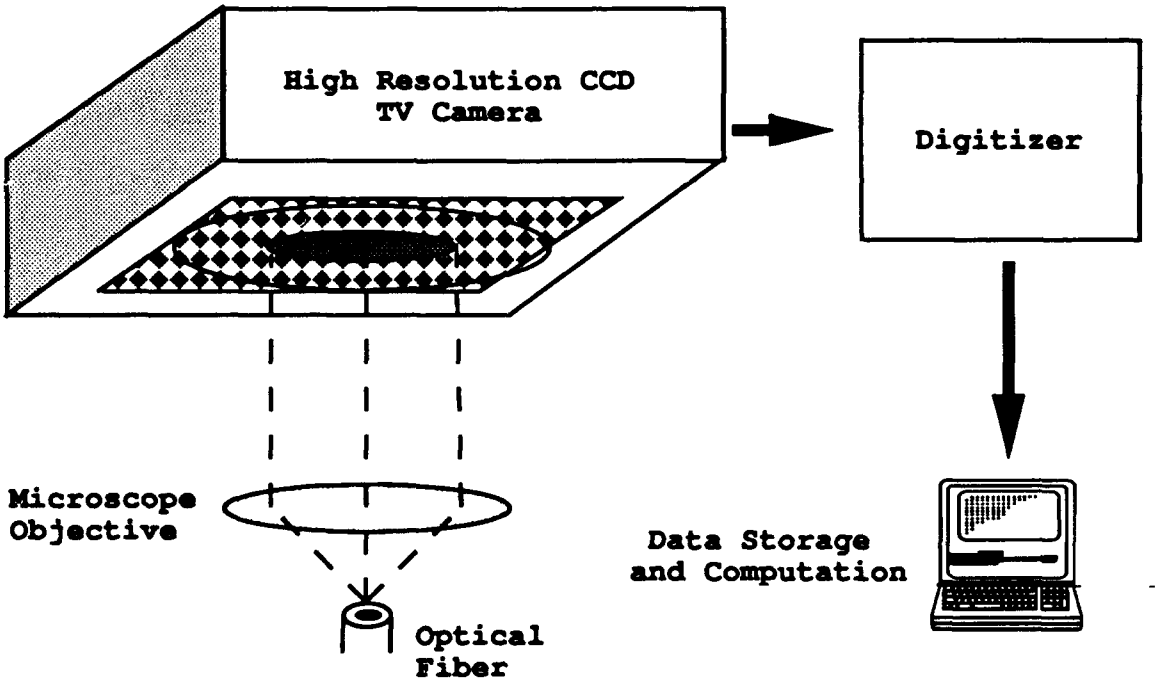

Figure 1. Near Field Pattern Measurement System

The optical power exiting the fiber is imaged onto the CCD array using a high-powered, large numerical aperture

microscope objective. For example a 40X, 0.65NA microscope objective could be used to image a 100/140μm, 0.3NA fiber. The fiber endface must be cleaved or polished to a minimum cleave angle and the fiber endface should contain no flaws. The CCTV camera must accurately measure the optical power as a function of position, and therefore must maintain linearity and minimize distortion. The CCTV output signal is then digitized and stored. Since axial symmetry is assumed, the near field pattern used in equation (6) is only a function of radial position. Therefore, if the entire two-dimensional NFP is measured, the center must be calculated and the data averaged and stored as a function of the radius. Otherwise, the NFP can be measured linearly across a diameter of the fiber. Again, the fiber center must be calculated and the data averaged and stored as a function of the radius. There are several methods available to calculate the center of the fiber. One method calculates the fiber's "center-of-mass". The fiber center is then given by:

$$x_o = \frac{\int N(r)\, x\, dx}{\int N(r)\, dx}, \quad y_o = \frac{\int N(r)\, y\, dy}{\int N(r)\, dy} \tag{28}$$

A second method calculates the position of all points of the NFP which are of equal radiance (e.g. 10% of the maximum radiance). This ring of positions is then fit to a circle of the form:

$$(x - x_o)^2 + (y - y_o)^2 = r_o^2 \tag{29}$$

where x_o, y_o describe the position of the fiber's center. Both of these methods have one-dimensional analogues should the NFP be measured in a single dimension across the fiber's diameter. Further information regarding the measurement of the Near Field Pattern can be found in FOTP-43, "Output Near-Field Radiation Pattern Measurement of Optical Waveguide Fibers."

Modal Power Distribution Calculation

In order for the Modal Power Distribution to be calculated using equation (5), the fiber radius and refractive index profile must also be determined. The fiber core radius should be measured using FOTP-58, "Core Diameter Measurement of Graded-Index Optical Fibers." Several methods exist to measure the refractive index profile of an optical fiber, some of which are outlined in Marcuse[13]. The refracted ray method is further described in FOTP-44, "Refractive Index Profile, Refracted Ray Method." For the purposes of this investigation a square-law profile fiber has been assumed. A calculation of the MPD requires differentiation of the near field pattern. Because of the noise inherent in any measurement of the NFP, direct differentiation results in an "amplification" of the noise such that the MPD becomes physically meaningless. Therefore, some type of smoothing operation must be performed on the NFP before differentiation. One suggested smoothing operation fits the NFP data to a linear combination of smooth functions before differentiation. Chebychev, Type II, $\{U_n(x)\}$ are the polynomials of choice for this investigation because they are complete and orthogonal over a range [-1,+1] and have a weighting function with a functional dependence resembling the refractive index profile

$$w(x) = (1-x^2)^{1/2} \qquad (30)$$

which accelerates convergence. The linear combination of functions is truncated after the fitted polynomials have sufficiently converged to the NFP data. Differentiation can be accomplished algebraically given the known[14] recursion relation

$$(1-x^2)\,U_n'(x) = -n\,x\,U_n(x) + (n+1)\,U_{n-1}(x) \qquad (31)$$

Mode Selective Excitation

In order for the 2x2 transition matrix of a passive fiber optic component to be calculated using equation (23), the input and output modal power distributions must be calculated for two, linearly independent input conditions. A ray of light incident on the fiber cross section at a radius r and angle θ with respect to the normal, excites a mode of the propagation constant:

$$\frac{\delta}{\Delta} = \frac{r^2}{a^2} + \frac{\sin^2\theta}{(NA)^2} \tag{32}$$

Graphing lines of constant propagation constant yields the phase-space diagram illustrated in Figure 2.

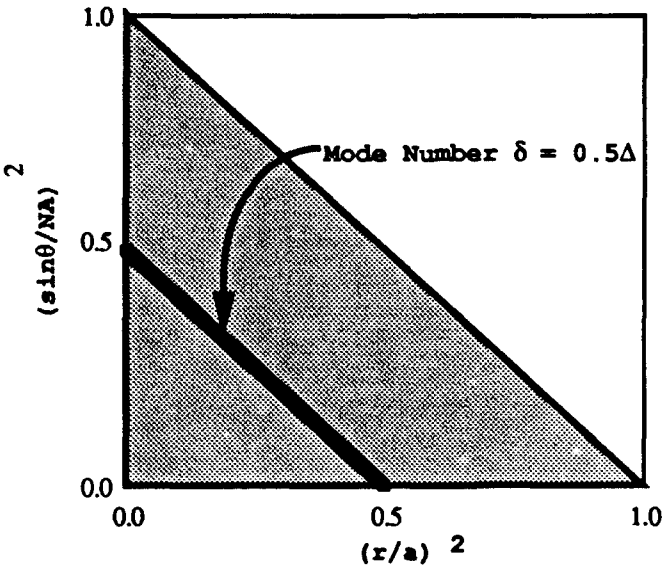

Figure 2. Phase-space diagram for parabolic-index optical fiber.

The guided modes of the fiber are represented by the shaded region of the diagram. Phase-space diagrams can be used

effectively to calculate the modal power distribution for various launch conditions.

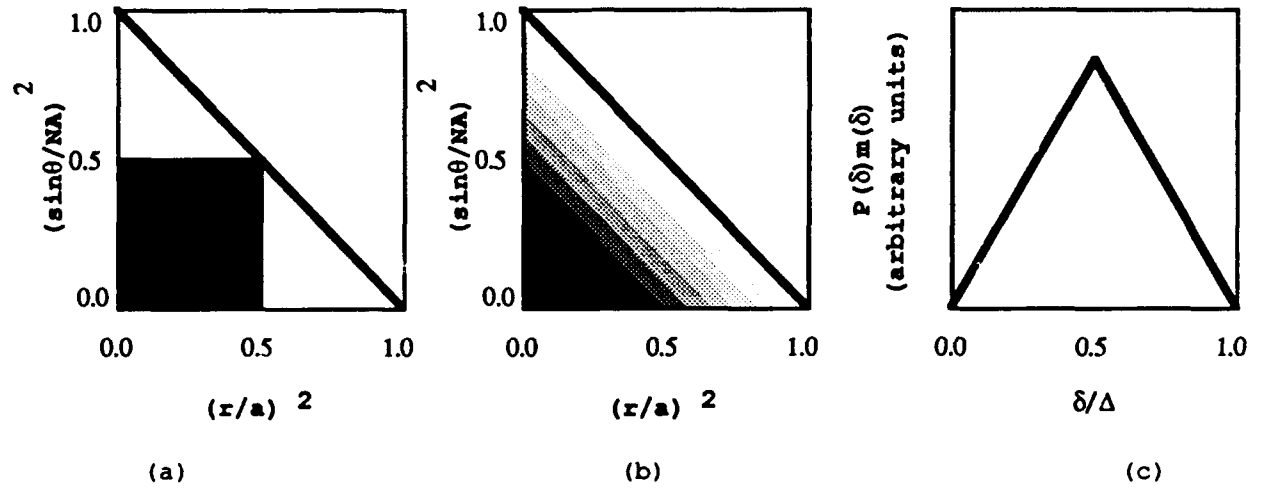

Figure 3. (a) Modes excited by an uniform spot r=0.7, sinθ=0.7, (b) Modes excited in test fiber allowing for coupling between nearly degenerate modes, and (c) resulting Modal Power Distribution.

Figure 3a shows the phase-space diagram for an underfilled, uniform, spot excitation. The spot is assumed to be of a diameter equal to 0.7 the diameter of the fiber under test. The numerical aperture is also assumed to be 0.7 the NA of the fiber under test. The power is assumed to become uniformly distributed between modes of constant mode number after propagating a "short" distance into the fiber, therefore the power propagating in each mode must be averaged between all of the modes of the same propagation constant as illustrated in Figure 3b. The product, $P(\delta)m(\delta)$, entering the test fiber is calculated by integrating the optical power along lines of constant δ. The resultant is illustrated in Figure 3c. As we can see, the underfilled spot excitation excites a predominantly "low-order" mode group. The phase-

space diagram and $P(\delta)m(\delta)$ of a uniformly overfilled fiber are illustrated in Figure 4a and Figure 4b.

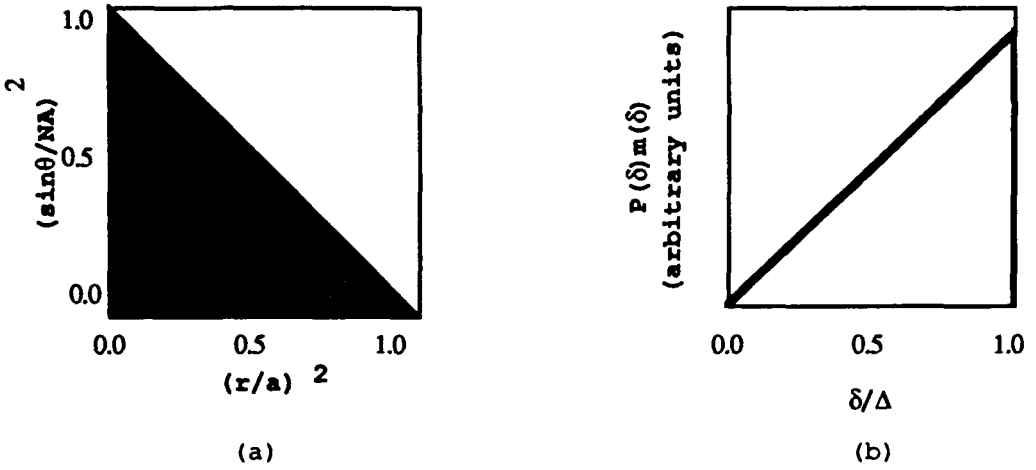

Figure 4. Modes excited by a uniform spot r=1.0, sinθ=1.0, and (b) resulting Modal Power Distribution.

An overfilled spot launch (r=a, sinθ=NA) excites a predominantly "high-order" modal power distribution. Therefore, we have determined that the input modal power distributions generated from underfilled and overfilled spot excitations are linearly independent. A mode selective launcher which generates these two input conditions is illustrated in Figure 5.

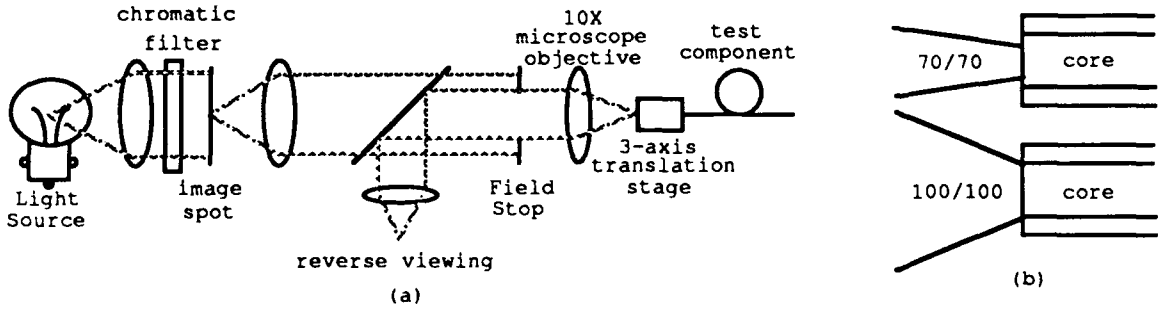

Figure 5. (a) Mode Selective Launch System, and (b) Underfilled and Overfilled Launches

An incoherent source illuminates an adjustable spot which is imaged using two microscope objectives onto the endface of the optical fiber. The concentricity of the spot and fiber is assured by viewing the fiber endface through a beamsplitter which is introduced between the objectives. An adjustable field stop is also placed between the objectives for the purpose of selecting the input numerical aperture. Agarwal, et. al.[15] discuss mode-selective excitation methods in considerable detail and give several alternative methods to the one aforementioned.

FOUR PORT POWER SPLITTER

(experimental comparison of loss prediction methods)

A comparison of loss measurement methods was made using a four-port power splitter which was fabricated by concatenating three 1x2, 3dB power splitters as illustrated in Figure 6.

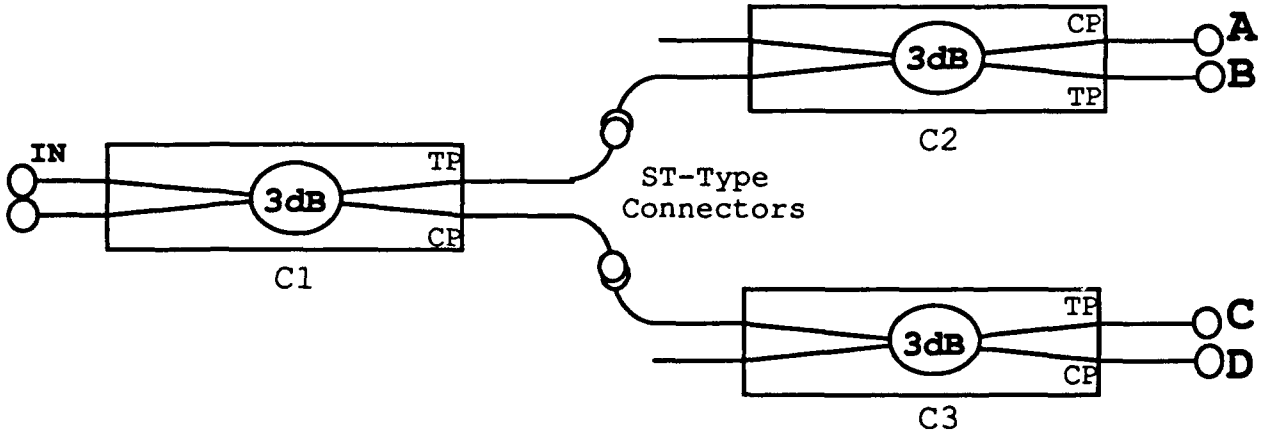

Figure 6. Four-port power splitter fabricated from serial 3dB power splitters. illustrating the through ports (TP) and coupled ports (CP) for the individual splitters: C1, C2, and C3.

Each power splitter was connectorized using ST-type connectors. Table 1 presents the measured mode transition matrices of the individual splitters (a) and the matrix for each output port of the concatenation (b). The predicted concatenated matrices, obtained by multiplying the individual component matrices in reverse order of their physical sequence, are also presented for comparison (c). The predicted values are in good agreement with the measured values. The input power vectors for the two independent launch conditions were measured and were found to be $\overline{P}_L$ = [0.801, 0.199] for the underfilled launch and $\overline{P}_H$ = [0.469,

0.531] for the overfilled launch. Predicted loss values of the concatenation were calculated using three methods. The first of these, Method 1, assumes the loss of the concatenation can be described by the addition of the loss values of the individual components measured using an overfilled launch. This would be the predicted value if FOTP 34 Method A were used to characterize the components.

$$\begin{bmatrix} 0.742 & -0.033 \\ -0.056 & 0.485 \end{bmatrix}_{TP} \quad \begin{bmatrix} 0.792 & -0.059 \\ -0.051 & 0.516 \end{bmatrix}_{TP} \quad \begin{bmatrix} 0.784 & -0.034 \\ -0.056 & 0.488 \end{bmatrix}$$

C1 C2 C3

$$\begin{bmatrix} 0.250 & 0.086 \\ 0.118 & 0.421 \end{bmatrix}_{CP} \quad \begin{bmatrix} 0.178 & 0.065 \\ 0.092 & 0.345 \end{bmatrix}_{CP} \quad \begin{bmatrix} 0.191 & 0.083 \\ 0.125 & 0.387 \end{bmatrix}$$

(a)

$$\begin{bmatrix} 0.098 & 0.032 \\ 0.064 & 0.164 \end{bmatrix} \quad A \quad \begin{bmatrix} 0.128 & 0.026 \\ 0.049 & 0.164 \end{bmatrix}$$

$$\begin{bmatrix} 0.567 & -0.055 \\ -0.055 & 0.247 \end{bmatrix} \quad B \quad \begin{bmatrix} 0.591 & -0.055 \\ -0.067 & 0.252 \end{bmatrix}$$

$$\begin{bmatrix} 0.146 & 0.049 \\ 0.071 & 0.197 \end{bmatrix} \quad C \quad \begin{bmatrix} 0.192 & 0.053 \\ 0.044 & 0.201 \end{bmatrix}$$

$$\begin{bmatrix} 0.079 & 0.036 \\ 0.074 & 0.186 \end{bmatrix} \quad D \quad \begin{bmatrix} 0.058 & 0.052 \\ 0.077 & 0.174 \end{bmatrix}$$

(b) (c)

Table 1. Mode Transition Matrices for (a) 1x2, 3dB power splitters, (b) 1x4, 6dB power splitters, (c) calculated concatenation outputs from multiplied matricies.

The second method, Method 2, assumes the concatenated loss can be described by the addition of the loss values of the individual components measured using an underfilled launch. This would be the predicted value if FOTP 34 Method B were

used to characterize the components. Finally, Method 3 assumes the concatenated loss can be determined from the multiplication of the power vector by the mode transition matrix of each component in reverse order of its physical sequence. Assuming a detector response vector of unity, the optical loss is given by:

$$\text{loss (dB)} = -10 \cdot \log\left(\frac{\bar{1} \cdot \bar{\bar{T}}_2 \cdot \bar{\bar{T}}_1 \cdot \bar{P}_{in}}{\bar{1} \cdot \bar{P}_{in}}\right) \text{ where } \bar{P}_{in} = \begin{pmatrix} P_1 \\ P_2 \end{pmatrix} \text{ and } \bar{1} = (1, 1) \qquad (30)$$

The measured and predicted loss values for each optical port and both launch conditions are given in Table 2.

PORT	Measured Loss (dB)		Predicted Loss (dB)			
			Method 1	Method 2	Method 3	
	Overfill	Underfill			Overfill	Underfill
A	7.46	7.75	7.15	7.20	7.35	7.46
B	4.58	3.42	4.83	3.62	4.55	3.38
C	6.35	6.53	5.91	5.75	6.10	6.21
D	7.25	7.82	7.51	8.59	7.37	8.15

TABLE 2. Measured and predicted loss values for 1x4 power splitter fabricated from three 1x2 power splitters. The predicted values were calculated using three methods: 1) additive overfilled losses, 2) additive underfilled losses, and 3) mode transition matrix technique.

The discrepancies between measured and predicted loss values can be calculated for each method. Averaging the discrepancies for each method between ports, and assuming the uncertainty of the method to be given by the standard deviation of the discrepancies between ports we get the

discrepancy values listed in Table 3. All three methods accurately predict the average loss of the concatenation for a launch condition similar to the one used in the method. In other words, the average loss through the four ports of the concatenation can be determined accurately (average discrepancy < 0.1dB) for an overfilled launch if Method 1 or 3 is used, while the average loss of an underfilled launch can be predicted accurately if either Method 2 or 3 is used.

	Discrepancy Between Measured and Predicted Loss (dB)	
	Overfill Launch	Underfill Launch
Method 1	-0.03 ± 0.34	-0.24 ± 1.30
Method 2	-0.39 ± 1.00	-0.08 ± 0.54
Method 3	-0.07 ± 0.13	-0.01 ± 0.19

Table 3. Discrepancy between measured and predicted values averaged between optical ports with an uncertainty equal to the standard deviation between optical ports.

Method 3 predicts the average loss of both launch conditions accurately because it inherently takes into account some of the modal properties of the passive network. This is one of the advantages of the matrix approach. In system design, however, the loss must be predicted accurately for each port, not just the average loss through all ports. Therefore we must examine the deviations reported in Table 3. The underfilled loss method does not accurately predict the concatenated loss of each port for either launch condition,

and therefore, should not be used. The overfilled loss measurement method predicts the loss of the concatenation for an overfilled launch sufficiently well (deviation < 0.5dB), but can not predict the loss of the underfilled concatenation. The matrix method, however, can predict the loss of each port very well (deviation < 0.2dB) for either launch condition. It is this predictive capability which is the main advantage of the matrix method.

MTM MEASUREMENT SYSTEM

Introduction

The usefulness of the mode transition matrix method has been demonstrated in predicting the loss of a concatenation of fiber optic components. The technique, however, is inherently complicated, requiring a measurement of the near field pattern as well as the total optical power both entering and exiting the device under test for two independent excitation conditions. These measurements require expensive equipment such as a CCD array or CCTV camera and the data must be processed using complicated mathematical operations such as curve fitting, differentiation, and integration. In the following sections, an invention (NAVY CASE NO. 73670) is described which allows the Mode Transition Matrix of a passive fiber optic component to be determined quickly and accurately using a novel method which does not require the measurement of a near field pattern. The invention only requires an ability to measure the total optical power entering and exiting the component, and all calculations are limited to algebraic operations involving matrices, which are simple in comparison to differentiation and curve fitting routines.

Alternative Basis Sets

Previously, orthogonal step functions $\{\phi_1(\delta), \phi_2(\delta)\}$ were described and used because of their physical significance. While it is desirable to retain the descriptiveness of such a basis set, other basis sets may be more convenient and adaptable to measurement procedures. It has been shown that the coupling of modes in a fiber optic component can be written as a matrix equation (17) for an orthogonal step function basis described by equation (25) where the input and output power vectors are described by equation (26). If a second basis is chosen $\{\phi'_1(\delta), \phi'_2(\delta)\}$ and the power vectors $\bar{P}'^{i}, \bar{P}'^{o}$ are obtained using this basis set then a matrix equation can be written

$$\bar{P}'^{o} = \bar{\bar{T}}' \cdot \bar{P}'^{i} \tag{31}$$

The power vectors calculated using the step function basis are related to the power vectors calculated in this second basis by a matrix transformation

$$\bar{P} = \bar{\bar{c}} \cdot \bar{P}' \tag{32}$$

where the matrix elements are determined from

$$\phi_j(\delta) = \sum_{k=1}^{2} c_{jk}\, \phi_k(\delta) \tag{33}$$

Since the second basis set is not complete, this equality can not be unconditionally satisfied for all δ. If nothing is known or assumed about the modal power distributions entering or exiting the device under test, equation (33) can be solved

in a least squares sense. The solution for $\bar{\bar{c}}$ is then determined to be

$$\bar{\bar{c}} = \bar{\bar{\alpha}} \cdot \bar{\bar{\beta}}^{-1} \tag{34}$$

where

$$\alpha_{ij} = \int_0^{\Delta} \phi_i(\delta)\, \phi_j'(\delta)\, d\delta \quad \text{and} \quad \beta_{ij} = \int_0^{\Delta} \phi_i'(\delta)\, \phi_j'(\delta)\, d\delta \tag{35}$$

However, if the functional form of the modal power distributions is known or assumed then a better estimate for $\bar{\bar{c}}$ can be obtained from

$$\bar{\bar{c}} = \bar{\bar{P}} \cdot \bar{\bar{P}}'^{-1} \quad \text{where } \bar{\bar{P}} = \begin{pmatrix} P_1^i & P_1^o \\ P_2^i & P_2^o \end{pmatrix} \text{ and } \bar{\bar{P}}' = \begin{pmatrix} P_1'^i & P_1'^o \\ P_2'^i & P_2'^o \end{pmatrix} \tag{36}$$

where the modal power vector components are calculated using the assumed input and output MPDs. In either case, given this transformation matrix, $\bar{\bar{c}}$, the transition matrix calculated using orthogonal step functions, $\bar{\bar{T}}$, is related to the transition matrix calculated using the second basis set, $\bar{\bar{T}}'$, by

$$\bar{\bar{T}} = \bar{\bar{c}} \cdot \bar{\bar{T}}' \cdot \bar{\bar{c}}^{-1} \tag{37}$$

The invention to be described uses mode filters and fiber optic switches to selectively measure the power vectors and mode transition matrix of a non-orthogonal basis set. The basis set can be determined using phase space diagrams, and the transformation matrix, $\bar{\bar{c}}$, calculated either using equation (34) or (36). The mode transition matrix described by equation (27) can then be determined using equation (37).

Description and Operation

The functional diagram of the invention is illustrated in Figure 7.

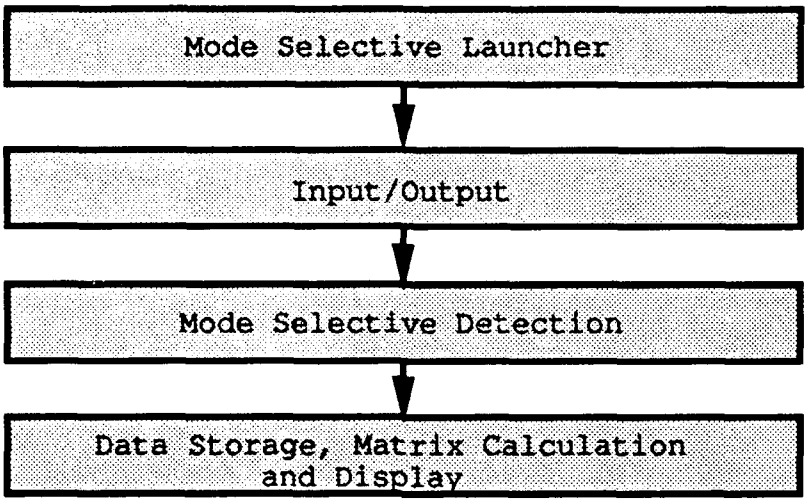

Figure 7. Functional Diagram of Matrix Measurement System.

The device can be broken into four major sections, 1) mode selective launcher, 2) input/output optics, 3) mode selective detector, and 4) data storage and matrix calculation software. The four sections will be discussed independently. For the purposes of this report, the device under test is assumed to be made of 100/140μm, 0.3NA optical fiber, operating at a wavelength of 850nm. However, a device fabricated with any size optical fiber operating at any wavelength could be used provided all fiber sizes, source, and detection devices mentioned in this report are scaled appropriately.

Mode Selective Launcher: The mode selective launcher is illustrated in Figure 8.

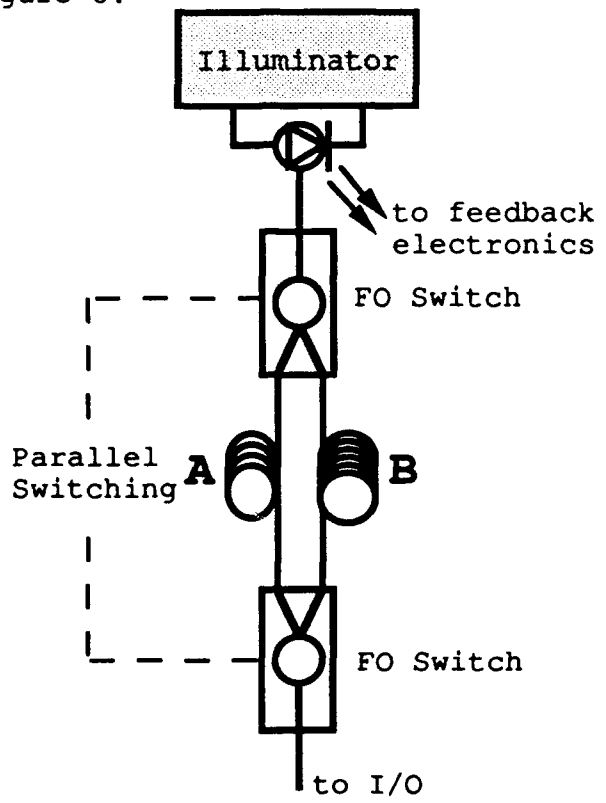

Figure 8. Mode Selective Launcher

The launching device consists of a pigtailed, high-power 850nm light emitting diode (any LED that overfills the 100/140µm fiber), and two 100/140µm fiber optic switches (Dicon Fiberoptics #S-12-L-100-ST-P or the like), operated in unison, to provide selection between two optical paths. The LED must be maintained at a constant optical output power throughout the duration of the measurement (the time scale could vary between a few seconds and a few minutes depending on whether or not a microprocessor has been used for control). A typical feedback circuit to maintain constant

optical power is illustrated in Figure 9, but any like circuit may be used without failure.

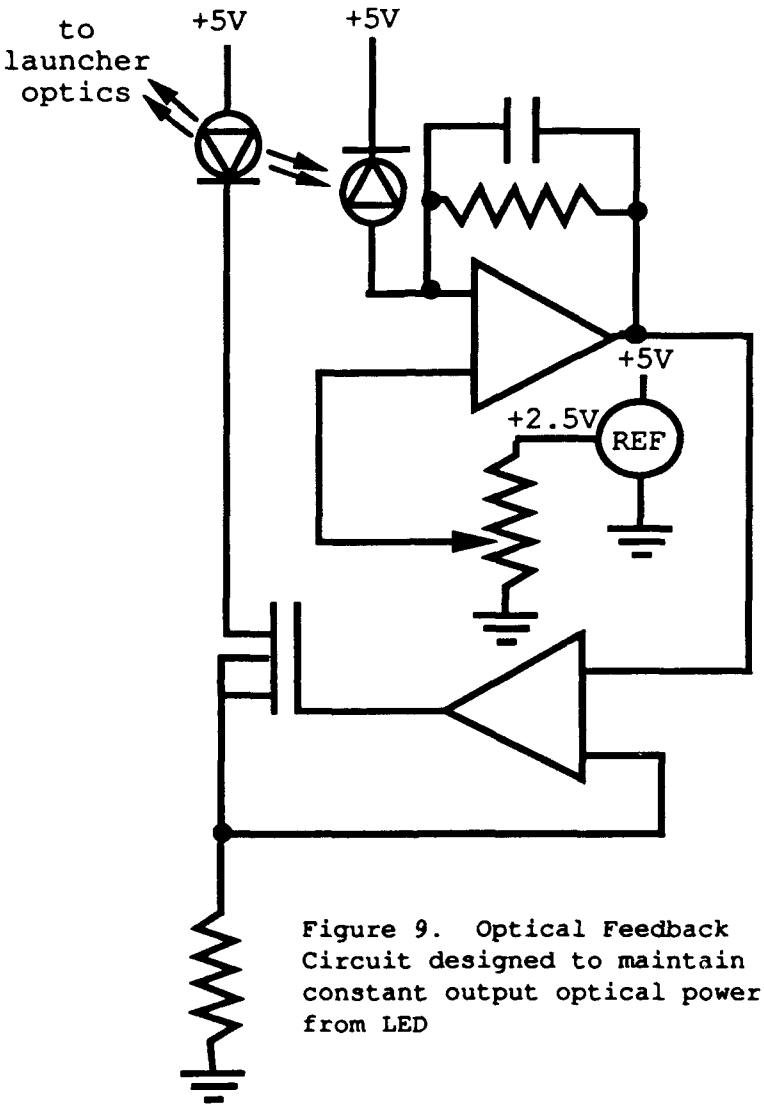

Figure 9. Optical Feedback Circuit designed to maintain constant output optical power from LED

The first path, A, consists of a short piece of a 'small-core' (e.g. 50/125μm, 0.2NA) optical fiber. The purpose of this fiber is to selectively filter high-order modes from the device under test. The low-pass characteristics of this undersized fiber are illustrated in Figure 10a. The second path, B, contains a mode mixer. This mode-mixing fiber

should provide an overfilled mode distribution (all guided modes contain power) to the device under test as illustrated in Figure 10b.

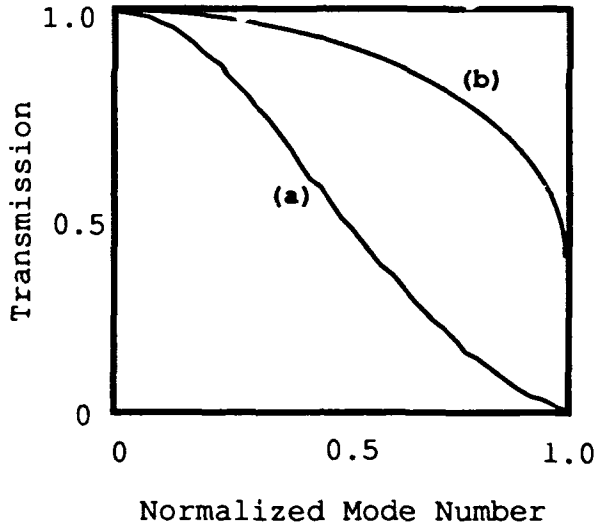

Figure 10. (a) Mode Filter Selectively passes low-order modes, and (b) Mode Mixer overfills fiber.

Therefore, this section of the invention allows the user to switch between underfilled and overfilled launch conditions.

Input/Output Optics: The input/output optics section consists of two fiber optic switches, which are operated in unison to provide the user a selection between two optical paths as illustrated in Figure 11.

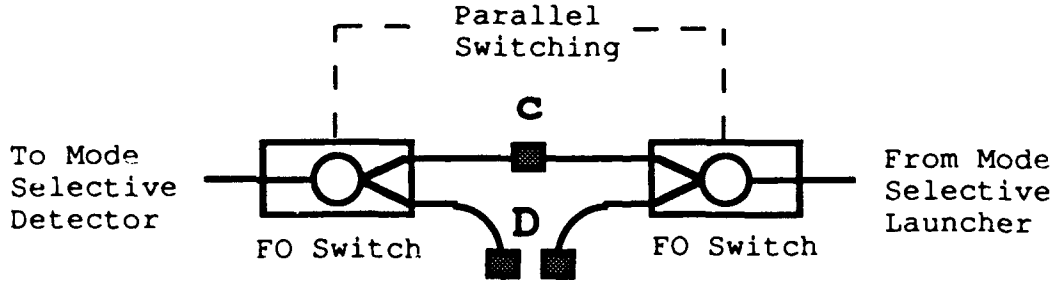

Figure 11. Input/Output for Measurement System.

The first path, C, contains nothing more than the outputs of the fiber switches terminated with fiber optic connectors which are mated to each other (e.g. ST-type connector). The second path, D, contains the outputs of the fiber switches terminated with similar fiber optic connectors which are to be mated to the device under test. This section therefore provides user selection of an optical path through a reference fiber containing a single connector or through the device under test.

Mode Selective Detection: The mode selective detection section is similar in design to the mode selective launcher and is illustrated in Figure 12.

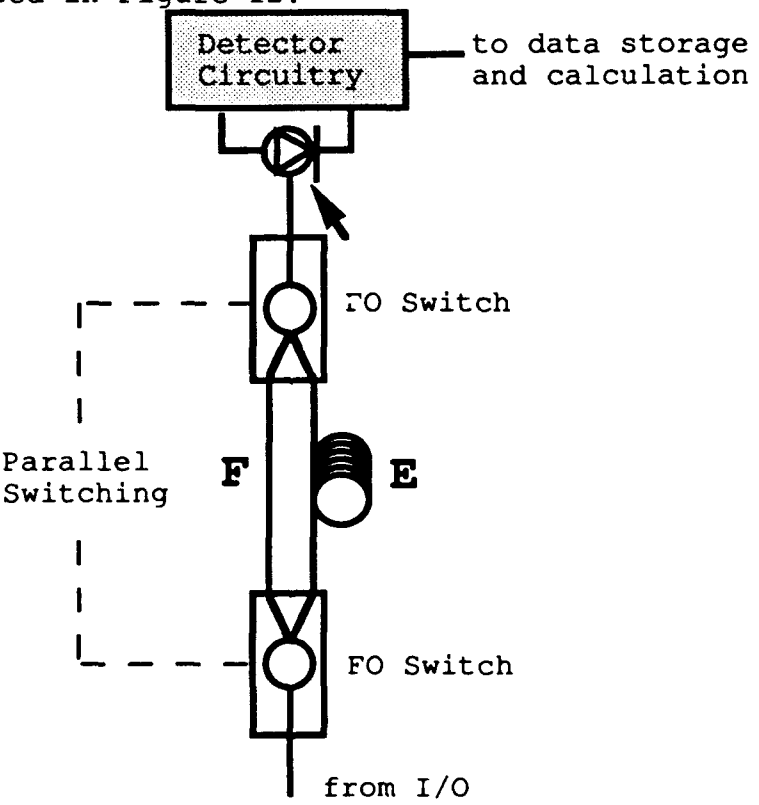

Figure 12. Mode Selective Detector

Again, two fiber optic switches are used in unison to select between two optical paths. The first path, E, again contains a short piece of undersized, 50/125μm, optical fiber to filter the high-order modes. The second path, however, contains no additional fiber, and merely provides an uninterrupted path to the detector. The detector must be large enough in area to collect all of the light exiting the 100μm optical fiber, and must be stable for the time duration of the measurement. A power meter, such as the Photodyne Model 22XLC with a model 150 Silicon Detector Head, can be used for power measurements, and offers the advantage of a large dynamic range. The mode selective detector allows the user to measure the power in two independent mode groups. The first group contains predominantly low-order modes, while the second contains all guided modes.

Data Storage and Matrix Calculation:

Figure 13 illustrates the general scheme for the Mode Transition Matrix Measurement system. The device consists of three sets of fiber optic switches. The first set is incorporated into the launch optics and can switch the optical path between paths A and B of Figure 8. The second set is part of the input/output optics and switches the optical path between paths C and D of Figure 11. The final set of switches is found in the detector optics and switches the optical path between paths E and F of Figure 12. The three sets of switches allow $2^3=8$ total independent optical

paths. A measurement of the optical power which propagates through each of these paths must be measured and recorded. For convenience I shall denote these power measurements by P_{xyz}, where x describes the launch optical path and can have the values A or B, y describes the input/output optical path

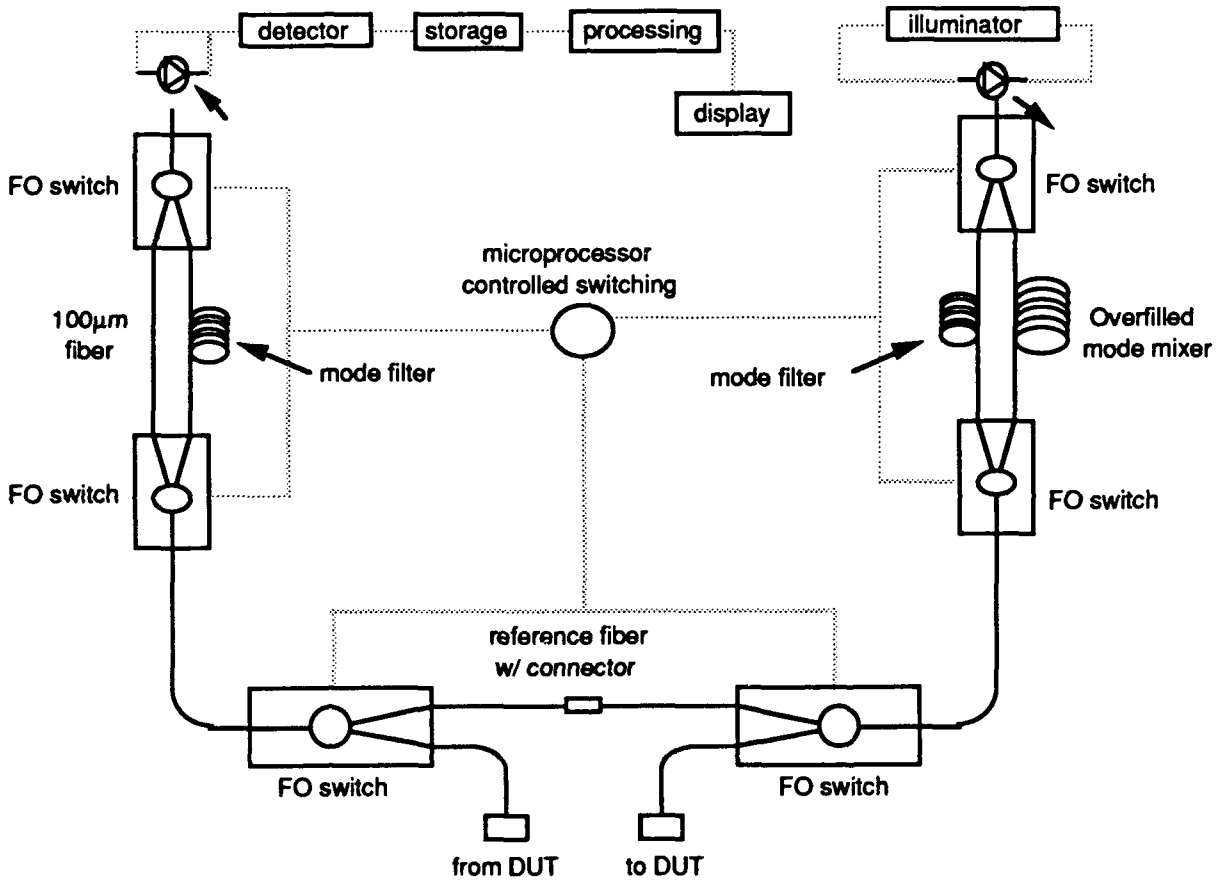

Figure 13. Microprocessor controlled Matrix Measurement System

and can have the values C or D, and z describes the detector optics and can have the values E or F. Then the eight power measurements can be recorded as P_{ACE}, P_{BCE}, P_{ADE}, P_{BDE}, P_{ACF}, P_{BCF}, P_{ADF}, P_{BDF}. These power measurements can be grouped into two, 2x2 matrices. The first shall be called the "Input Matrix" and is a description of the power which propagates

through the reference fiber. The second is called the "Output Matrix" and describes the power which propagates through the Device Under Test (DUT). The Input and Output matrices are then defined as:

$$\bar{\bar{I}} = \begin{bmatrix} P_{ACE} & P_{BCE} \\ P_{ACF} & P_{BCF} \end{bmatrix} \quad \bar{\bar{O}} = \begin{bmatrix} P_{ADE} & P_{BDE} \\ P_{ADF} & P_{BDF} \end{bmatrix} \tag{38}$$

With these measured values the component's matrix can be calculated by multiplying the matrices according to:

$$\bar{\bar{T}}' = \bar{\bar{O}} \cdot \bar{\bar{I}}^{-1} \tag{39}$$

where $\bar{\bar{T}}'$ is the component's matrix measured relative to the mode groups selected by the invention. The mode transition matrix, $\bar{\bar{T}}$, is related to $\bar{\bar{T}}'$ by the similarity transformation of equation (37). The transformation matrix, $\bar{\bar{c}}$, can be either theoretically determined from a description of the fiber used in the mode filters, or measured experimentally.

Transformation Matrix c: The transformation matrix, $\bar{\bar{c}}$, "rotates" the optical power vector measured using the MTM Measurement system into the power vector which would be measured using the conventional mode block representation. As discussed previously, the transformation matrix can be determined in either of two methods.

The first method assumes nothing is known about the functional form of the modal power distributions entering and exiting the device under test. The method solves equation

(33) in a least squares sense. The solution, presented as equation (34), requires a determination of the basis set which describes the mode filters used in the selective detection unit of the MTM measurement system. This can be accomplished using the phase-space diagrams illustrated in Figure 14.

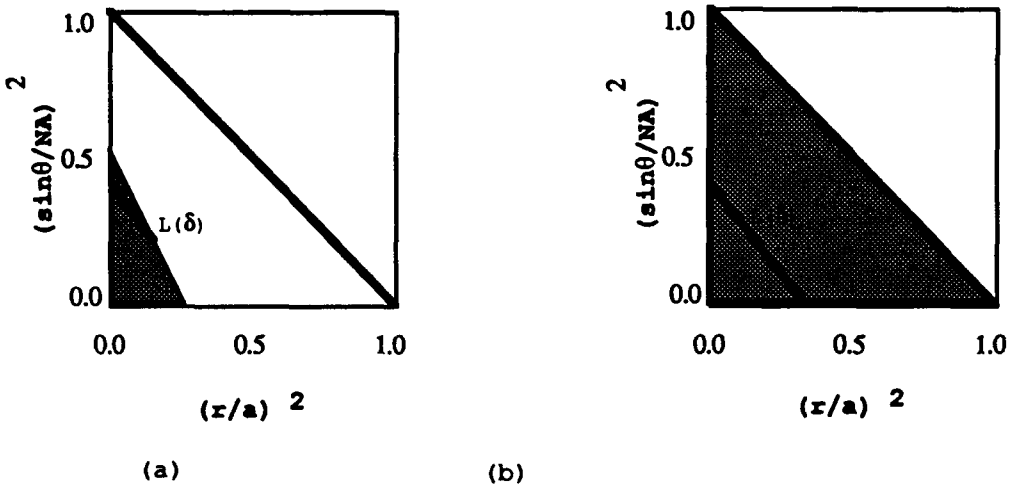

Figure 14. (a) The modes transmitted by an undersized fiber mode filter in a 100/140μm fiber. (b) The guided modes of a 100/140μm fiber.

Path E contains a piece of "small-core" fiber as described previously. For the purposes of the following calculations, this mode filtering fiber is assumed to be 50/125μm, 0.20NA graded-index fiber. The area of the large triangles represents all of the guided modes of a 100/140μm, 0.29NA graded-index optical fiber. The shaded triangular region of Figure 14a represents the portion of the power which will be transmitted through the mode filter. The length of the diagonal line, $L(\delta)$, is proportional to the fractional power allowed through path E for a given mode number δ and is determined geometrically to be

$$L(\delta) = \begin{cases} \sqrt{2}\,\delta, & \delta < \frac{1}{4}\Delta \\ \sqrt{2}\,(\frac{1}{2} - \delta), & \delta > \frac{1}{4}\Delta, \delta < \frac{1}{2}\Delta \\ 0, & \delta > \frac{1}{2}\Delta \end{cases} \tag{40}$$

The basis function, $\phi'_1(\delta)$, is calculated by dividing this length by $\sqrt{2}\delta$ in order to account for the density of modes. Therefore for this mode filter we have determined the basis function to be

$$\phi_1'(\delta) = \begin{cases} 1, & \delta < \frac{1}{4}\Delta \\ \frac{1}{2\delta} - 1, & \delta > \frac{1}{4}\Delta, \delta < \frac{1}{2}\Delta \\ 0, & \delta > \frac{1}{2}\Delta \end{cases} \tag{41}$$

The second basis function is easier to obtain. Since path F of the mode selective launcher transmits all the optical power regardless of mode number, the basis function is given by

$$\phi_2'(\delta) = 1 \quad \text{for all} \quad \delta \tag{42}$$

The transformation matrix can now be determined from equation (34) and equation (35) and is given by

$$\bar{\bar{c}} = \begin{pmatrix} 0.706 & 0.232 \\ -0.706 & 0.768 \end{pmatrix} \tag{43}$$

It is interesting to note that if a 70μm, 0.2NA graded-index fiber were used in path E then the mode filter basis function would equal the low-order mode block basis function. The equality of equation (33) could then be unconditionally satisfied for all δ, and therefore the transition matrix $\bar{\bar{T}}$ could be determined exactly.

The second method requires a knowledge of the modal power distributions entering and exiting the device under test. If it is assumed that all power vectors transform under the same transformation matrix, $\bar{\bar{c}}$, then the transformation matrix can be determined using equation (36). This is illustrated in Figure 15. Figure 15a is a phase-space diagram in which the shaded region represents the fiber modes which contain optical power in a 100/140μm fiber which has been excited by a 50/125μm step-index fiber. If we project this shaded region of unit intensity onto the low- and high-order mode blocks of Figures 10c and 10d, then we obtain a power vector in the mode block representation equal to $P_A = [1.0, 0.0]$. Similarly if we project the shaded region of Figure 15b, which shows a uniformly overfilled mode distribution, onto these mode blocks we obtain a power vector given by $P_B = [0.25, 0.75]$. These are the power vectors obtained in the mode block representation. It is a slightly more subtle argument to determine the power vectors as would be measured by the MTM measurement system. Figure 16 illustrates the problem. The mode-filtered launch is again illustrated in Figure 16a. The modes which lie along a diagonal are of the same radial mode number and are therefore nearly degenerate. It has been assumed that the optical power is strongly coupled between these modes, and therefore the power contained in the square becomes uniformly distributed along these diagonal modes as seen in Figure 16b. Path E of the

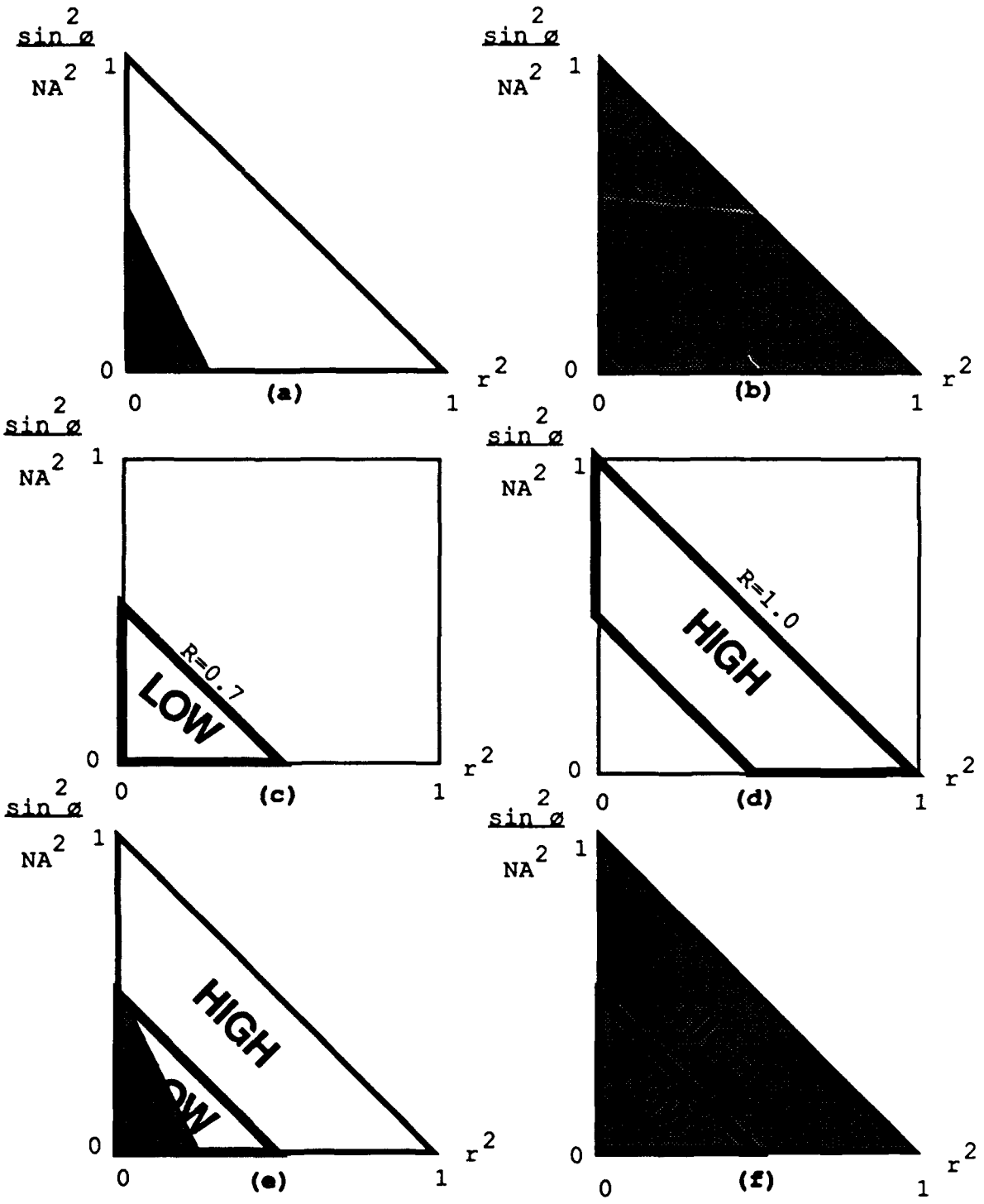

Figure 15. Modes propagating optical power in (a) underfilled launch, and (b) over filled launch; (c) low-order mode block, and (d) high-order mode block; projection of (e) underfilled launch, and (f) overfilled launch onto mode blocks.

mode selective detector measures the power which is contained in the triangular group of modes illustrated in Figure 16c.

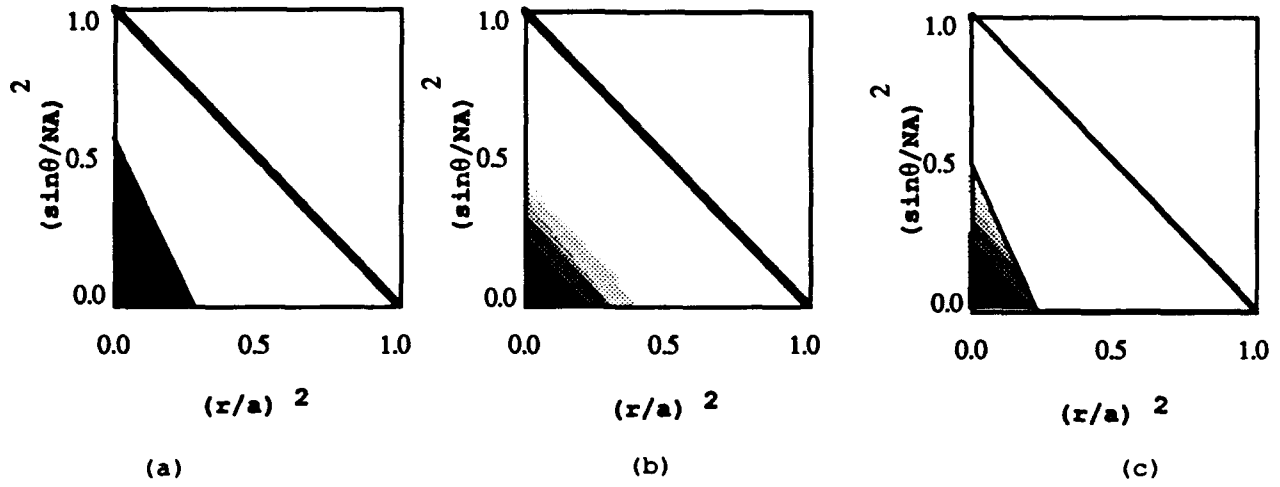

Figure 16. (a) The modes excited by an undersized fiber mode filter in a 100/140μm fiber. Strong coupling between degenerate modes averages the power along diagonals (b). The mode filter in the mode selective detector filters many of the higher-order modes (c).

Therefore, in order to determine the power vector measured by the MTM Measurement system, the launched mode block must be projected onto the detector mode block after allowing for the averaging of power among degenerate modes. This is a subtle point, and results in power vectors for the two launch conditions: $P_A' = [0.8215, 1.0]$, $P_B' = [0.125, 1.0]$. The second coefficient of each vector is unity because Path F of the mode selective detector allows all fiber modes a continuous path to the detector. From these power vectors, the transformation matrix can be calculated.

$$\overline{\overline{C}} = \left[\overline{P_A} \quad \overline{P_B} \right] \cdot \left[\overline{P_A}' \quad \overline{P_B}' \right]^{-1}$$

$$= \begin{bmatrix} 1.00 & 0.25 \\ 0.00 & 0.75 \end{bmatrix} \cdot \begin{bmatrix} 0.8215 & 0.125 \\ 1.0 & 1.0 \end{bmatrix}^{-1}$$

$$= \begin{pmatrix} 1.072 & 0.116 \\ -1.072 & 0.884 \end{pmatrix} \quad (44)$$

This matrix differs only slightly from the matrix determined using the basis functions. It is important to note that any matrix $\bar{\bar{c}}' = a \cdot \bar{\bar{c}}$, where a is any constant, will yield the same transition matrix, $\bar{\bar{T}}$, because the similarity transformation requires the multiplication of $\bar{\bar{T}}'$ by both $\bar{\bar{c}}$ and $\bar{\bar{c}}^{-1}$.

Use for Pigtailed Optical Sources: In order to measure the modal power vector of a pigtailed optical source, the mode selective detector is used as a 'stand-alone' unit. The connectorized pigtail of the optical source is mated to the detector input connector. A single pair of optical switches provides two independent power measurements, P_L and P_H, where the subscripts correspond to low-order and high-order detection. The two measurements are arranged into a column vector and then multiplied by the transformation matrix, $\bar{\bar{c}}$, to yield the input power vector, $\bar{P}_i$, which can be used in system performance predictions.

Experimental Results

The mode transition matrix of the coupled port of the fiber optic power splitter labeled C1 in Figure 6, page 24, was determined using the mode transition matrix measurement system. The input and output power matrices of equation (38) are given in Table 4, together with the calculated matrix, $\bar{\bar{T}}'$. This matrix was transformed using the two transformation

$$I = \begin{bmatrix} 80.54 & 74.64 \\ 96.83 & 319.2 \end{bmatrix}$$

$$O = \begin{bmatrix} 17.70 & 26.61 \\ 32.66 & 131.2 \end{bmatrix}$$

$$T' = \begin{bmatrix} 0.166 & 0.044 \\ -0.123 & 0.440 \end{bmatrix}$$

(a)

(b) $\begin{bmatrix} 0.230 & 0.104 \\ 0.077 & 0.376 \end{bmatrix}$

(c) $\begin{bmatrix} 0.233 & 0.079 \\ 0.105 & 0.375 \end{bmatrix}$

(d) $\begin{bmatrix} 0.250 & 0.086 \\ 0.118 & 0.421 \end{bmatrix}$

Table 4. (a) Input and Output Power matricies and the resultant Transition Matrix measured using The MTM Measurement System. (b) and (c) MTMs calculated from the similarity transformations using the transformation matrices described in Equations (43) and (44) respectively, and (d) MTM calculated from a measurement of the Near Field Patterns entering and exiting the device under test (reproduced from Table 1).

matrices given in equations (43) and (44). The results are presented in Table 4 together with the Mode Transition Matrix determined previously using the Near Field Pattern technique. There is good agreement between the matrix values for all cases.

ALTERNATIVE APPROXIMATION TECHNIQUES

There are several alternate methods to characterize the modal characteristics of multimode fiber optic components. Two other methods which deserve mention are 1) differential mode attenuation, and 2) mode transfer function.

Differential Mode Attenuation

In some passive fiber optic components, it is possible that there is little coupling between modes of different propagation constant. In this case, the mode transfer function, $T(\delta,\delta')$ can be written as

$$T(\delta,\delta') = \begin{pmatrix} T(\delta) & \delta = \delta' \\ 0 & \delta \neq \delta' \end{pmatrix} \tag{45}$$

The integration over δ' of equation (14) can now be done yielding a solution of the form

$$T(\delta) = \frac{P^o(\delta)}{P^i(\delta)} \tag{46}$$

This is a very special case of the general problem, and it must be determined experimentally which optical components can be described with this method.

Mode Transfer Function

The functional form of the transfer function of equation (14) might be deduced from a knowledge of the properties of the fiber optic component. For example, in a low-loss fiber optic connector, Yang, et al[3] assume that a Gaussian coupling function exists

$$T(R,R') = \delta(R-R') - \int dR'' \, m(R'')\alpha(R'',R)\delta(R-R') + m(R)\alpha(R,R') \tag{47}$$

where

$$\alpha(R,R') = \frac{1}{2}\alpha_o e^{-\frac{|R^2-R'^2|}{2\tau}} \tag{48}$$

where α_o and τ are fitting parameters (R is the mode parameter to avoid confusion with the delta-function), which can be determined from a measurement of the loss and the near field patterns entering and exiting the device under test for a single excitation. Mode transition matrices can be generated from this transfer function for any basis set using equation (18). The limitations of this technique lie in one's ability to accurately assume, *a priori*, a form for the transfer function of complicated passive fiber optic devices.

COMPUTER SOFTWARE

Three computer programs have been written to support the mode transition matrix investigation. The first program stores the digitized near field pattern data together with the total optical power and the fiber radius. The near field pattern data is then fit to a linear combination of user chosen basis functions using a curve fitting program. The two basis sets presently available are Chebychev and Hermite polynomials. This second program also differentiates the near field pattern fit algebraically using the well known recursion relations for these polynomial functions, and then calculates the modal power distribution from this derivative. Finally, the program integrates the modal power distribution into modal power vectors and records the coefficients. The third program calculates the mode transition matrix of the device under test from the modal power vectors associated with the input and output near field patterns of two independent excitation conditions. All programs have been written in Rocky Mountain BASIC for use by an HP 9826 laboratory computer.

Also available from the author is a program which calculates the fiber radius from the near field pattern. The program requires the NFP for an overfilled launch condition and calculates the radius from the -16dB points.

CONCLUSIONS

The mode transition matrix method has been determined to be a useful method to characterize the mode coupling present in passive fiber optic components. The experimental method, however, is quite complicated and requires much computational analysis. Input and output near field pattern data must be recorded for two independent launch conditions and then differentiated to calculate the modal power distribution. Because direct differentiation results in amplification of the noise inherent in the measured data, a smoothing routine or curve fitting operation must be applied. Through the use of fiber optic switches and mode filters, an optical system has been designed which can quickly and easily approximate the mode transition matrix. The method requires only the total optical power entering and exiting the device under test be recorded, and all mathematical operations are limited to algebraic operations of matrices. A patent disclosure has been submitted on the device (Navy Case # 73670). Other techniques exist which allow a description of the modal properties of fiber optic components. Two of these methods, differential modal attenuation and mode transfer function, were discussed. The assumptions made by each method as well as their limitations were presented.

REFERENCES

1. Daido, Y., Miyauchi, E., Iwama, T., and Otsuka, T., "Determination of Modal Power Distribution in Graded-Index Optical Waveguides From Near-=Field Patterns and its Application to Differential Mode Attenuation Measurements," *Applied Optics*, **18**, 13, 1979.

2. Holmes, G.T., "Estimation of Concatenated System Response Based on Measured Transfer Functions for Low and High Order Modes," *Proc. 7th European Conference on Optical Communication*, Copenhagen, 1981.

3. Yang, S., Vayshenker, I.P., Hjelme, D.R., and Mickelson, A.R., "Transfer Function Analysis of Measured Transfer Matrices," *Applied Optics*, **28**, 15, 1989.

4. Evers, G., Kober, A., and Unrau, U., "Measurement of Mode Transition Matrices of Quasi-Step-Index Optical Fiber Components," *SPIE Vol. 500 Fiber Optics: Short-Haul and Long-Haul Measurements and Applications II*, 1984.

5. Vayshenker, I.P., Hjelme, D.R., and Mickelson, A.R., "Multimode Fiber Systems Characterization," *Technical Digest: Symposium on Optical Fiber Measurement, NBS Special Publication 720*, 1986.

6. Eriksrud, M., Mickelson, A.R., Aamlid, S., and Espe, B., "*Mode Dependence of Splice Loss in Graded-Index Optical Fibers*," IEEE Journal of Quantum Electronics, **19**, 5, 1983.

7. Gabriel, C.J., "Transfer Matrices for Multimode Optical Fiber Systems," *Naval Ocean Systems Center: Technical Document 1717*, 1989.

8. Gryk, T.J., Holmberg, G.E., Blount, H.M., "Sensitivity of the Mode Transition Matrices to Variations of the Input Power Vectors," *Technical Digest: Symposium on Optical Fiber Measurements, NBS Special Publication 748*, 1988.

9. Grau, G.K., and Leminger, O.G., "Relations Between Near-Field and Far-Field Intensities, Radiance, and Modal Power Distribution of Multimode Graded-Index Fibers," *Applied Optics*, **20**, 3, 1981.

10. Leminger, O.G., and Grau, G.K., "Near-Field Intensity and Modal Power Distribution in Multimode Graded-Index Fibres," *Electronics Letters*, **16**, 17, 1980.

11. Mickelson, A.R., and Eriksrud M., "Mode-Continuum Approximation in Optical Fibers," *Optics Letters*, **7**, 11, 1982.

12. Unrau, U.B., "Mode Transition Matrix Techniques for Multimode Fiber-Optic Components," *Technical Digest: Symposium on Optical Fiber Measurements*, NBS Special Publication 748, 1988.

13. Marcuse, D., *Principles of Optical Fiber Measurement*, Academic Press, Inc., New York, 1981.

14. Arfken, G., *Mathematical Methods For Physicists*, Academic Press, Inc., New York, 1966.

15. Agarwal, A.K., Evers, G., Unrau, U., "A Measurement Set-Up for Differential Mode Analysis of Fiber-Optic Components," *ntzArchiv* (Germany), **8**, 9, 1986.

INITIAL DISTRIBUTION LIST

Addressee	No. of Copies
NOSC (Harris Quesnell, Code 753; Richard Walker, Code 7502)	2
DTIC	2